Robust handling of extremes in quantile mapping - "Murder your darlings"

Peter Berg[1], Thomas Bosshard[1], Denica Bozhinova[1], Lars Bärring[1], Joakim Löw[1], Carolina Nilsson[1], Gustav Strandberg[1], Johan Södling[1], Johan Thuresson[1], Renate Wilcke[1], and Wei Yang[1]

[1]Swedish Meteorological and Hydrological Institute, Folkborgsvägen 17, 601 76 Norrköping, Sweden

Correspondence: Peter Berg (peter.berg@smhi.se)

Abstract. Quantile mapping is a method often used for bias adjustment of climate model data toward a reference, i.e. to construct a transformation of the model's distribution to that of the reference. The main moments of the distributions are typically well transformed by quantile mapping, but statistical uncertainty increases towards the extreme tails, making robust transformations challenging. Because of the limited data at the extreme tails, also an empirical quantile mapping needs to make some estimation or fit a parameterized function for data beyond the calibration data range. The MIdAS bias adjustment platform is here employed to explore different methods for handling the extreme tail, which are evaluated using an indicator for extreme precipitation - the maximum daily precipitation amount per year. Different methodologies are evaluated for a large ensemble of regional climate model projections over Scandinavia. The sensitivity of the empirical quantile mapping for the tails of the distribution is demonstrated, and it is found that the behaviour is significantly different within and without the calibration period, causing severe issues with the temporal consistency of the timeseries. The sensitivity is identified to be due to differences in the activated features of the bias adjustment, within the calibration period where the empirical transfer function is applied, and outside that period, where the extrapolation method is likely applied. This means that the bias adjustment method is in a sense different between different time periods. Currently MIdAS uses separate calibrations for each day of the year, as opposed to e.g. for each calendar month, which further aggravates this issue. Further, finding a robust parametrisation for the tail is not straightforward. We identify a two-step solution which works well for this problem: (i) "murder your darlings" by excluding data from the tail data in the calibration period, the extrapolation feature is activated for all time periods, even the calibration period, and (ii) applying an outlier insensitive method for linear regression works well for finding an extrapolation parametrisation for the tail.

1 Introduction

Bias adjusted climate projections are routinely used for impact modelling, and further processed into climate indicators for various climate services. Climate indicators of extremes are, by definition, sensitive to the small sample, which becomes even more sensitive when combined with reference data to map a transformation in the bias adjustment step. Such sensitivity can impose large uncertainties in the interpretation and conclusions drawn from the extreme indicator, and in the worst case rendering the information useless or even misleading.

Many bias adjustment methods are based on the quantile mapping approach, where a transfer function is used to map model data in different quantiles of a distribution to match that of the reference data set, see further detailed descriptions in Berg et al. (2022). Earlier studies have identified issues with bias adjusting data outside the calibration range for pure empirical quantile mapping approaches (Boé et al., 2007; Bellprat et al., 2013). A common solution is to apply the adjustment value of the high end of the calibration period for all data outside the calibration range (Themeßl et al., 2011), although this may introduce unrealistically large adjustments (Switanek et al., 2017). A combination of empirical and parametric approaches have been proposed by several authors, e.g. by using extreme value theory fits to the top 5% data (Tani and Gobiet, 2021), while others have applied linear fits to the extremes (Holthuijzen et al., 2022).

Clearly, a purely empirical method based on all data in the calibration period might act differently when applied outside the calibration data range compared to its calibration. The method reacts to data outside the calibration range differently to inside the range, e.g. re-using the highest adjustment value of the calibration range (Themeßl et al., 2011), which means that the behaviour of the bias adjustment differs depending on the magnitude of the values that are adjusted. In other words, the bias adjustment method differs for data inside and outside the calibration range. This may lead to unexpected results for the bias adjusted tails. One can force the bias adjustment to apply its full behaviour only by making sacrifices at the very tail of the distribution. In a way similar to the literary method of "Murder your darlings" (Quiller-Couch, 2015), also known as "kill your darlings", i.e. to remove the most precious items for the greater good of the work: "Whenever you feel an impulse to perpetrate a piece of exceptionally fine writing, obey it—whole-heartedly—and delete it before sending your manuscript to press. Murder your darlings."

This paper presents a clear example of problematic side effects of bias adjustment within and outside the calibration period. A new method to handle the calibration strategy and distribution fits to the tail is presented and tuned to find a pragmatic use of data while reducing the side-effects. The example is based on data from the Swedish climate service, using a large ensemble of regional climate models and the MIdAS bias adjustment method (Berg et al., 2022).

2 Bias adjustment

The MIdAS implementation of quantile mapping starts from the quantile-quantile (Q-Q) plots of the reference and model data sets, which share the same number of data points. A piece-wise linear smoothing spline function is fitted to the Q-Q plot, see Berg et al. (2022) for details. MIdAS applies a linear function fitted to the 90% most central data points of the Q-Q plot, with weights defined by the standard deviation of the data points from the linear fit. A linear continuation of the spline is applied to data points outside of the calibration data range, i.e. a "$1-1$" linear continuation of the spline in the Q-Q plot, as explained in detail in (Berg et al., 2022).

The transfer functions are calculated based on a historical period, here 1971–2000, for each grid point and in sub-sets of the annual cycle. Rather than using calendar month sub-sets, as in most published methods, MIdAS is set up to calculate and apply the transfer functions based on the day of the year ($doy = [1, 365]$), using a moving window of 15 d before and after doy, such that 31 d times the number of calibration years are used to build the distribution of the reference and model data.

2.1 New parameterization for the tail

The new development to handle data at the tails of the distributions is based on the fitting procedure of Theil-Sen (Theil, 1950; Sen, 1968) which is an outlier insensitive method. The procedure is to calculate the median of slopes derived from each individual pair of points in the sample, i.e. in the Q-Q plot. It means that outliers will have little individual effect on the fits, making the linear fits robust to the high sample uncertainties that are unavoidable at the tail of the distributions. The Theil-Sen approach aligns with the general philosophy of MIdAS to use generally applicable methods that are not dependent on specific distributions. The reason for this philosophy is that MIdAS shall be transparent and equally applicable across geographic regions and climates without the need to pre-define specific distribution functions for each case.

When excluding high extreme data points in the calibration sample of precipitation, in order to activate extrapolation behaviour and the full bias adjustment method, there are unavoidable effects on other moments of the distribution. Because precipitation extremes often add significant quantities of precipitation, they are important in defining the mean moment. A balance between a good handling of extremes, and a good adjustment of the mean moment must be found.

Different versions of excluding data from the calibration data range are combined with the Theil-Sen regression on the top 5% data to find a balance between side-effects on the tail data and mainly the mean moment of the bias adjusted data:

- $R0T5$ - no excluded data and calibration on percentiles 95–100

- $R1T5$ - exclude 1% of the data on the upper tail and calibrate on percentiles 94–99

- $R5T5$ - exclude 5% on the upper end and calibrated on percentiles 90–95.

2.2 Data

Precipitation data from SMHIGridClim (Andersson et al., 2021) is used as reference data for the bias adjustment. SMHIGridClim is a data set based on the regional reanalysis UERRA (UERRA, 2019) combined with gauge data from Sweden and neighbouring countries, mapped at a 2.5 km grid and with daily temporal resolution. For this analysis, the data set is conservatively remapped (using first order conservative remapping following Jones (1998)) to the Euro-CORDEX 0.11 degree (approximately 12.5 km) grid covering Scandinavia.

The climate projections are acquired from the Euro-CORDEX CMIP5 data set (Jacob et al., 2020). A large ensemble of 67 unique combinations of global and regional models are used (see Table 1), using the RCP8.5 scenario of future emissions. The ensemble members all have bias to different extent both for the mean and the extreme tails, as evaluated for a sub-set of the ensemble in, e.g., Vautard et al. (2021).

2.3 Evaluation methods

Two statistics are used to evaluate the different methods in Sec. 2.1: the annual mean, and the annual maximum of daily precipitation. The mean is evaluated because it is summarizing the performance of the bias adjustment across all data, while the annual maximum highlights the most extreme values, that are specifically targeted in this study. Because the signal-to-
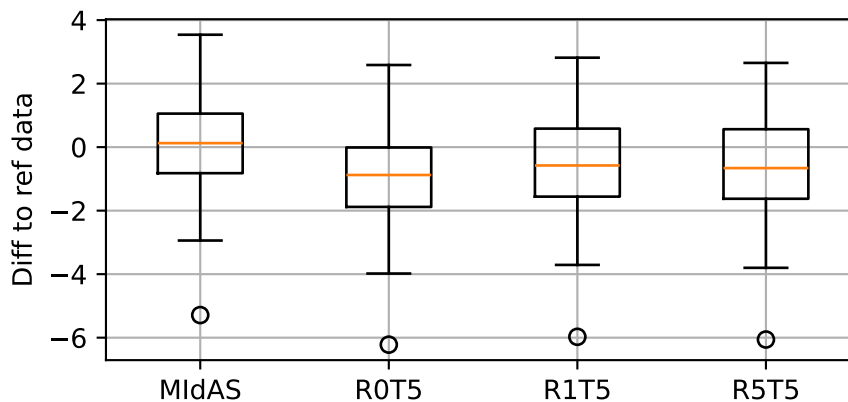
Figure 1. Remaining bias in the annual precipitation maxima (mm d^{-1}) for the ensemble members presented in a boxplot. Results are shown for the original MIdAS code and the different experiments.

noise levels are very high for the annual maxima, the ensemble mean is calculated across all members, and in addition a spatial
90 average is calculated over the land regions of the complete domain. The figures present the temporal evolution of ensemble mean for the the domain average annual mean and maxima.

3 Results

Figure 1 shows the performance of the different MIdAS setups for the annual maxima. The original MIdAS code is close to the reference data, which is expected as all the data points are included, and the deviations for different ensemble members is due
95 to how well the spline is fitted to the tail of the distribution. The different Theil-Sen methods show similar behaviour across the ensemble, but with a general underestimation of the annual maxima after bias adjustment. The remaining bias is on the order of less than 1 mm d^{-1} for the mean of the ensemble, which is less than o.5% relative bias. We consider this a sufficiently good fit, which does not urge for using more advanced fitting methods using extreme value theory.

Figure 2 shows the original ensemble result of annual maxima of daily precipitation averaged over the domain, together
100 with the reference data and the resulting bias adjusted data using the original implementation of MIdAS, as presented in Berg et al. (2022). In the calibration period, marked with vertical bars, the bias adjustment is efficiently offsetting the annual maxima to be at a similar level as the reference. Note that the interannual variability is reduced due to the ensemble averaging performed for the model data. However, outside the calibration period, there is almost no visible effect of the bias adjustment, resulting in significant discontinuities at the beginning and the end of the calibration period. This is clearly an issue, and is,
105 as will be shown, caused by the essentially different bias adjustment methods within (without extrapolation) and outside (with extrapolation) of the calibration period. The issue is very clearly seen in Fig. 2 because of the averaging over a larger domain. When assessed for single grid points or smaller domains, the issues are hidden within the large noise levels for this kind of
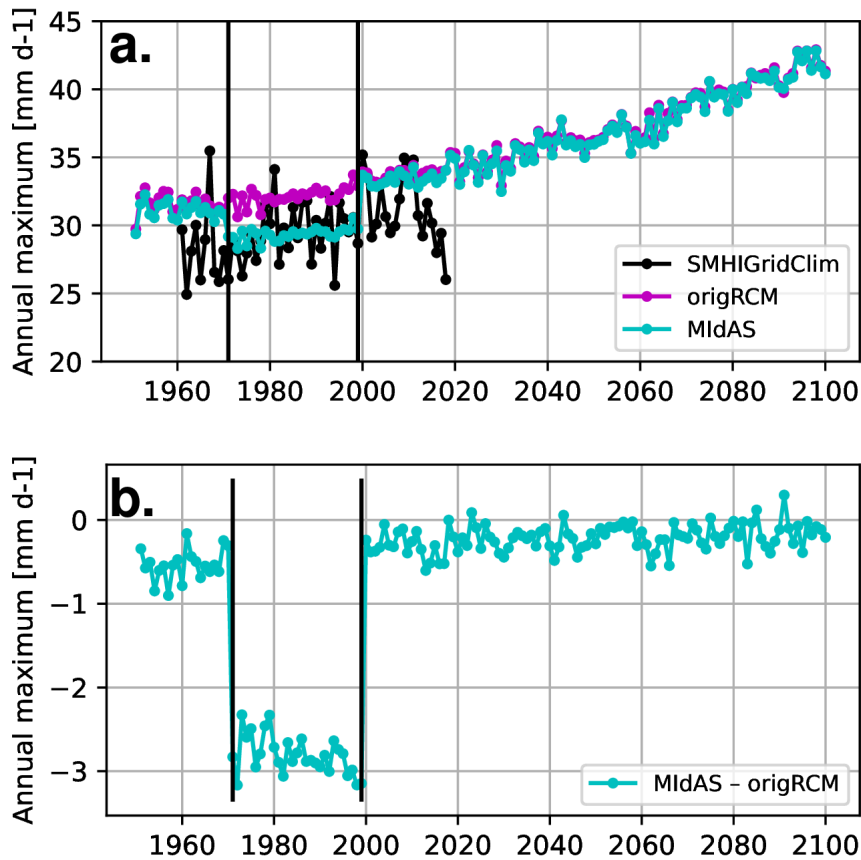
Figure 2. Annual precipitation maxima (mm d^{-1}) for SMHIGridClim, the original RCM ensemble mean, and the bias adjusted data using the standard MIdAS setup: for absolute levels (a), and for the difference between bias adjusted and original model data (b).

extreme precipitation statistics. This highlights the need to quality control and evaluate bias adjustment across larger areas, even though the parametrization and scale of the bias adjustment is intended for single grid points. Clearly, if the calibration period would also be used as a historical reference period, the climate change signal would be exaggerated by almost 3 mmd^{-1}, which is about twice the signal from the original data at mid-century.

In an attempt to improve on the performance outside the calibration period, the Theil-Sen method is applied to find a good fit to the top 5% data of the distribution (experiment R0T5), which is shown as a red line in Fig. 3. The adjustment within the calibration period is only mildly affected, due to the change from an assumed linear extrapolation in the original MIdAS method, and the Theil-Sen methodology. However, the main issue remains as there is still a significant offset at the beginning and the end of the calibration period.

Because the bias adjustment method will inevitably activate the extrapolation routine with data outside the calibration range, the next experiments (R1T5 and R5T5) force the extrapolation to be active also within the calibration range. In other words,
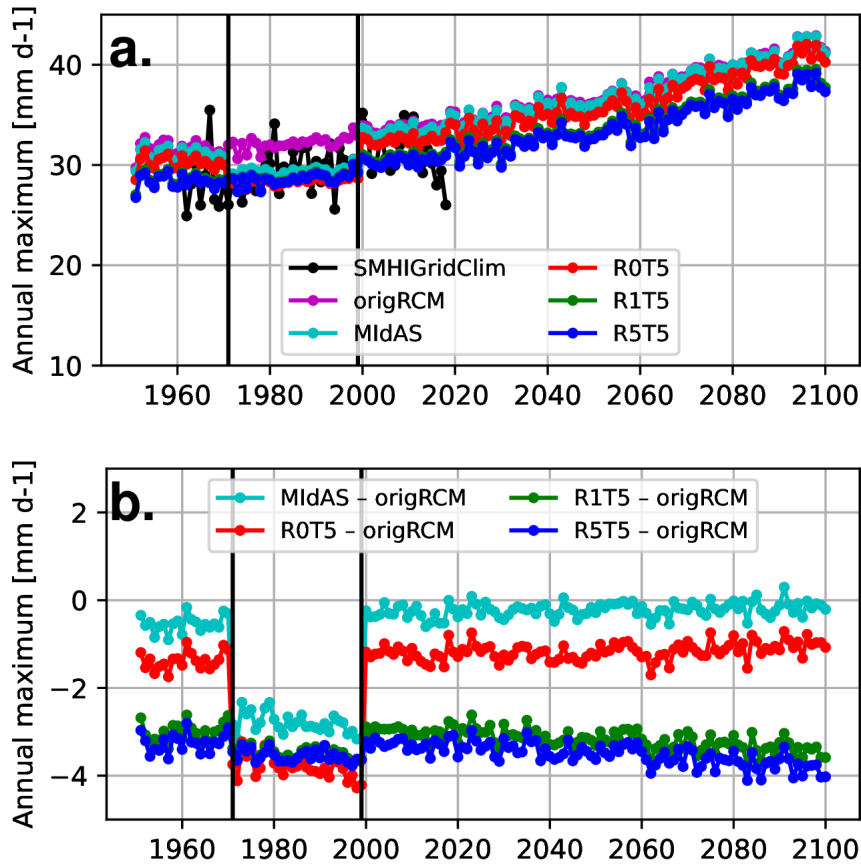
Figure 3. Same as Fig. 2, but with the additional data sets for the experiments R0T5, R1T5 and R5T5. Note that the green lines lies behind the blue line in panel a.

some extremes are excluded for the benefit of an overall better adjustment, at the likely cost of worse performance in the calibration period. Combining the Theil-Sen fit with exclusion of the top 5% of the calibration data (R5T5, blue) has a strong impact on the bias across the whole time series. The bias is still well adjusted in the calibration period, equal to the R0T5 experiment, but with the additional much improved performance outside the period. This result indicates that one can only reach a consistent bias adjustment across the time periods by activating the extrapolation routine for all periods, which implies disregarding of some tail data. In other words, by "murdering your darlings". Similar results are seen for the experiment R1T5 (green), where less data (1%) is excluded.

So what are the side-effects? The annual maxima is but one of many important aspects that the bias adjustment is supposed to improve, and often the more accumulated statistics such as the mean values are more important to reproduce. Figure 4 shows the annual sums of precipitation, i.e. the result on the accumulated precipitation of all intensities. While the original MIdAS method works well for this measure, the R5T5 method clearly imposes a dry bias. This is because a significant amount of
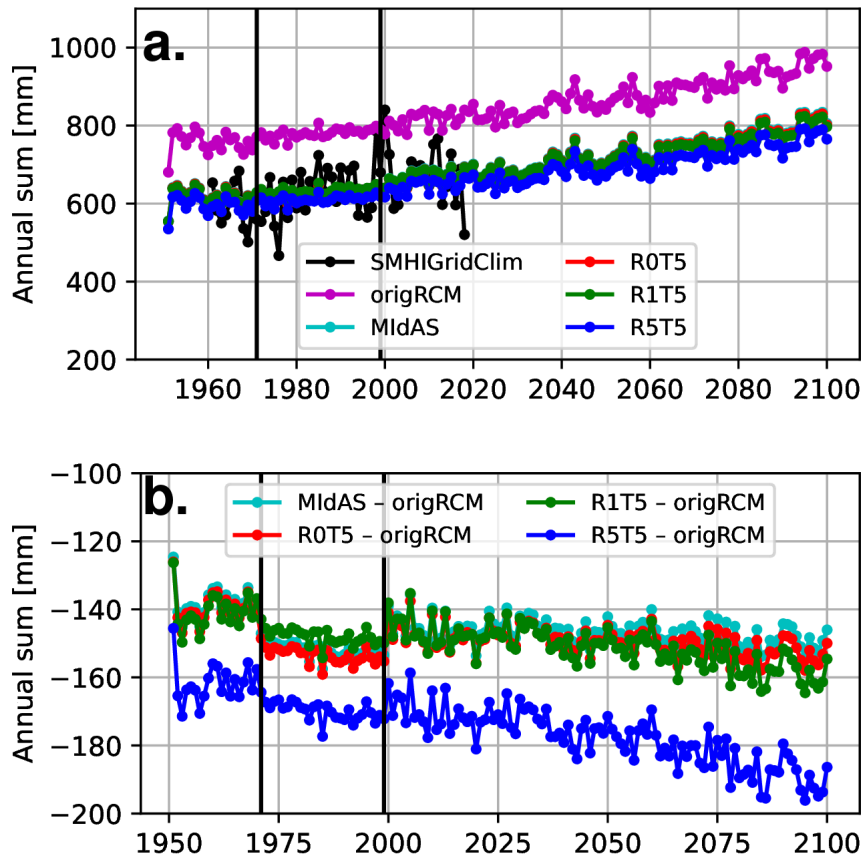
Figure 4. Same as Fig. 3, but for the annual sum of precipitation. Note that R0T5 is very close to R1T5 in panel a.

precipitation has been removed from the distribution in the calibration period (the 5% highest intensity events), which strongly impacts the overall bias. The sign of this impact depends on the original bias in the mean and the maximum precipitation. They are likely of the same sign as the maximum strongly affects the mean, but it may not always be that way. Reducing the exclusion of data to 1% (R1T5), the annual sums are closer to the reference data set, and the original method (Fig. 4, and as presented above, still resulting in a much similar result for the adjustment of the annual maxima (Fig. 3). However, Fig. 4 also highlights another important side-effect - a reduced trend of the increasing precipitation with time; most clearly seen in the difference plot Fig. 4b. This trend is seen for the original MIdAS, as well as all the experiments, although the impact seems significantly stronger for experiment R5T5. No significant impact on trends in annual maxima is seen for the original MIdAS adjustment and experiment R0T5, see Fig. 3b. However, when data are excluded in experiment R1T5 and R5T5, there is also an impact on the trends; much similar to that imposed on the mean statistic. One can debate whether this is a side-effect, or whether it is good to have consistent behaviour across the statistics, i.e. that the relative effects of the extremes and the means more closely follow each other in time.

4 Conclusions

This study focuses on an identified issue with bias adjustment of the highest extremes, which are adjusted differently within and outside the calibration period. A new outlier insensitive linear fit is used for the extreme tails, and a solution to the issue is presented in a set of experiments. The main conclusions are:

- The more extreme the statistic of interest is, the more elusive any bias becomes as the available data becomes scarcer and bias is a fundamentally statistical property. Therefore, to create a robust sample size the bias should be assessed over an ensemble of simulations and/or over a larger set of gridcells.

- A consistent bias adjustment method must have all features activated across all time periods, including the calibration period, in order to produce consistent bias adjustment.

- The extrapolation feature can be activated by excluding the highest data points in the calibration period, making sure that the extrapolation feature is acting on the complete time range, and result in consistent bias adjustment.

- An unavoidable trade-off between adjustment of the mean moment and the extremes is necessary, as excluding high intensity data points from the calibration will inevitably affect the mean.

- As there is an ever increasing focus on climate extremes we suggest that the performance of bias adjustment methods should routinely include an assessment of its impact on the extreme tails

Code and data availability. The MIdAS git repository is open for all to access and use under the GNU LESSER GENERAL PUBLIC LICENSE v3, at https://git.smhi.se/midas/midas. The code used for the final setup that handles the extreme tails is implemented in v0.3.0. The annual maxima and mean values, as well as Python scripts for reproducing the figures are available in Berg and Södling (2024).

Author contributions. PB – Conceptualization, Methodology, Formal analysis, Writing – Original Draft, Project administration, Funding acquisition; TB – Methodology, Software, (Writing – Review and Editing); LB – Methodology, (Writing – Review and Editing); JS – Methodology, Formal analysis, Investigation, Software, (Writing – Review and Editing); RW - Methodology, (Writing – Review and Editing); DB – Software, (Writing – Review and Editing); JL – Software, (Writing – Review and Editing); CN – Software, (Writing – Review and Editing); JS – Software, (Writing – Review and Editing); JT – Software, (Writing – Review and Editing); WY – Software, (Writing – Review and Editing); GS – Conceptualization, (Writing – Review and Editing), Project administration, Funding acquisition.

Competing interests. The authors declare that they have no conflicts of interest.

Acknowledgements. We acknowledge funding from the Swedish Meteorological and Hydrological Institute. Analyses were performed on the Swedish climate computing resource Bi provided by the Swedish National Infrastructure for Computing (SNIC) at the Swedish National Supercomputing Centre (NSC) at Linköping University. We acknowledge the work by Klaus Zimmermann in writing the base code, as presented in Berg et al. (2022), setting up the git repository, and much more.

170

References

Andersson, S., Bärring, L., Landelius, T., Samuelsson, P., and Schimanke, S.: SMHI Gridded Climatology, Tech. rep., Swedish Meteorological and Hydrological Institute (SMHI), 2021.

Bellprat, O., Kotlarski, S., Lüthi, D., and Schär, C.: Physical constraints for temperature biases in climate models, Geophys. Res. Lett., 40, 4042–4047, https://doi.org/https://doi.org/10.1002/grl.50737, 2013.

Berg, P. and Södling, J.: MIdAS bias adjustment of extremes using Theil-Sen extrapolation: Data and plotting scripts for GMD-publication, Tech. rep., Zenodo, https://doi.org/https://doi.org/10.5281/zenodo.12570891, 2024.

Berg, P., Bosshard, T., Yang, W., and Zimmermann, K.: MIdASv0.2.1 – MultI-scale bias AdjuStment, Geosci. Model Dev., 15, 6165–6180, https://doi.org/10.5194/gmd-15-6165-2022, 2022.

Boé, J., Terray, L., Habets, F., and Martin, E.: Statistical and dynamical downscaling of the Seine basin climate for hydro-meteorological studies, Int. J. Climatol., 27, 1643–1655, https://doi.org/10.1002/joc.1602, 2007.

Holthuijzen, M., Beckage, B., Clemins, P. J., Higdon, D., and Winter, J. M.: Robust bias-correction of precipitation extremes using a novel hybrid empirical quantile-mapping method, Theor. App. Climatol., 149, 863–882, https://doi.org/10.1007/s00704-022-04035-2, 2022.

Jacob, D., Teichmann, C., Sobolowski, S., Katragkou, E., Anders, I., Belda, M., Benestad, R., Boberg, F., Buonomo, E., Cardoso, R. M., Casanueva, A., Christensen, O. B., Christensen, J. H., Coppola, E., De Cruz, L., Davin, E. L., Dobler, A., Domínguez, M., Fealy, R., Fernandez, J., Gaertner, M. A., García-Díez, M., Giorgi, F., Gobiet, A., Goergen, K., Gómez-Navarro, J. J., Alemán, J. J. G., Gutiérrez, C., Gutiérrez, J. M., Güttler, I., Haensler, A., Halenka, T., Jerez, S., Jiménez-Guerrero, P., Jones, R. G., Keuler, K., Kjellström, E., Knist, S., Kotlarski, S., Maraun, D., van Meijgaard, E., Mercogliano, P., Montávez, J. P., Navarra, A., Nikulin, G., de Noblet-Ducoudré, N., Panitz, H.-J., Pfeifer, S., Piazza, M., Pichelli, E., Pietikäinen, J.-P., Prein, A. F., Preuschmann, S., Rechid, D., Rockel, B., Romera, R., Sánchez, E., Sieck, K., Soares, P. M. M., Somot, S., Srnec, L., Sørland, S. L., Termonia, P., Truhetz, H., Vautard, R., Warrach-Sagi, K., and Wulfmeyer, V.: Regional climate downscaling over Europe: perspectives from the EURO-CORDEX community, Reg. Environ. Change, 20, 51, https://doi.org/10.1007/s10113-020-01606-9, 2020.

Jones, P.: A User's Guide for SCRIP: A Spherical Coordinate Remapping and Interpolation Package, Version 1.4, Tech. rep., Los Alamos National Laboratory, 1998.

Quiller-Couch, A.: On the Art of Writing, Read Books Ltd, 2015.

Sen, P. K.: Estimates of the regression coefficient based on Kendall's tau, Am. Stat. Assoc. Bull., 63, 1379–1389, 1968.

Switanek, M. B., Troch, P. A., Castro, C. L., Leuprecht, A., Chang, H.-I., Mukherjee, R., and Demaria, E. M. C.: Scaled distribution mapping: a bias correction method that preserves raw climate model projected changes, Hydrol. Earth Syst. Sci., 21, 2649–2666, https://doi.org/10.5194/hess-21-2649-2017, 2017.

Tani, S. and Gobiet, A.: Quantile mapping for improving precipitation extremes from regional climate models, J. Agric. Meteorol., 21, 434–443, https://doi.org/10.54386/jam.v21i4.278, 2021.

Theil, H.: A rank-invariant method of linear and polynomial regression analysis, Indag. Math., 12, 173, 1950.

Themeßl, M. J., Gobiet, A., and Heinrich, G.: Empirical-statistical downscaling and error correction of regional climate models and its impact on the climate change signal, Clim. Change, 112, 449–468, https://doi.org/10.1007/s10584-011-0224-4, 2011.

UERRA: Complete UERRA regional reanalysis for Europe from 1961 to 2019, Tech. rep., Copernicus Climate Change Service (C3S) Climate Data Store (CDS), https://doi.org/10.24381/cds.dd7c6d66, (Accessed on 25-03-2024), 2019.

Vautard, R., Kadygrov, N., Iles, C., Boberg, F., Buonomo, E., Bülow, K., Coppola, E., Corre, L., van Meijgaard, E., Nogherotto, R., Sandstad, M., Schwingshackl, C., Somot, S., Aalbers, E., Christensen, O. B., Ciarlo, J. M., Demory, M., Giorgi, F., Jacob, D., Jones, R. G., Keuler, K., Kjellström, E., Lenderink, G., Levavasseur, G., Nikulin, G., Sillmann, J., Solidoro, C., Sørland, S. L., Steger, C., Teichmann, C.,
210   Warrach-Sagi, K., and Wulfmeyer, V.: Evaluation of the Large EURO-CORDEX Regional Climate Model Ensemble, J. Geophys. Res., 126, https://doi.org/10.1029/2019JD032344, 2021.

Table 1. List of the EURO-CORDEX GCM-RCM simulations included in the evaluation and the RIP (realisation-initialization-physics) code.

GCM	RCM	RIP	GCM	RCM	RIP
CCCma-CanESM2	CCLM4-8-17	r1i1p1	MOHC-HadGEM2-ES	ALADIN63	r1i1p1
CCCma-CanESM2	REMO2015	r1i1p1	MOHC-HadGEM2-ES	HIRHAM5	r1i1p1
CNRM-CERFACS-CNRM-CM5	COSMO-crCLIM-v1-1	r1i1p1	MOHC-HadGEM2-ES	REMO2015	r1i1p1
CNRM-CERFACS-CNRM-CM5	ALADIN63	r1i1p1	MOHC-HadGEM2-ES	RegCM4-6	r1i1p1
CNRM-CERFACS-CNRM-CM5	HIRHAM5	r1i1p1	MOHC-HadGEM2-ES	WRF381P	r1i1p1
CNRM-CERFACS-CNRM-CM5	REMO2015	r1i1p1	MOHC-HadGEM2-ES	RACMO22E	r1i1p1
CNRM-CERFACS-CNRM-CM5	WRF381P	r1i1p1	MOHC-HadGEM2-ES	HadREM3-GA7-05	r1i1p1
CNRM-CERFACS-CNRM-CM5	RACMO22E	r1i1p1	MOHC-HadGEM2-ES	RCA4	r1i1p1
ICHEC-EC-EARTH	COSMO-crCLIM-v1-1	r12i1p1	MPI-M-MPI-ESM-LR	COSMO-crCLIM-v1-1	r1i1p1
ICHEC-EC-EARTH	COSMO-crCLIM-v1-1	r1i1p1	MPI-M-MPI-ESM-LR	COSMO-crCLIM-v1-1	r2i1p1
ICHEC-EC-EARTH	COSMO-crCLIM-v1-1	r3i1p1	MPI-M-MPI-ESM-LR	COSMO-crCLIM-v1-1	r3i1p1
ICHEC-EC-EARTH	CCLM4-8-17	r12i1p1	MPI-M-MPI-ESM-LR	CCLM4-8-17	r1i1p1
ICHEC-EC-EARTH	HIRHAM5	r12i1p1	MPI-M-MPI-ESM-LR	ALADIN63	r1i1p1
ICHEC-EC-EARTH	HIRHAM5	r1i1p1	MPI-M-MPI-ESM-LR	HIRHAM5	r1i1p1
ICHEC-EC-EARTH	HIRHAM5	r3i1p1	MPI-M-MPI-ESM-LR	REMO2015	r3i1p1
ICHEC-EC-EARTH	REMO2015	r12i1p1	MPI-M-MPI-ESM-LR	RegCM4-6	r1i1p1
ICHEC-EC-EARTH	RegCM4-6	r12i1p1	MPI-M-MPI-ESM-LR	WRF381P	r1i1p1
ICHEC-EC-EARTH	WRF381P	r12i1p1	MPI-M-MPI-ESM-LR	RACMO22E	r1i1p1
ICHEC-EC-EARTH	RACMO22E	r12i1p1	MPI-M-MPI-ESM-LR	HadREM3-GA7-05	r1i1p1
ICHEC-EC-EARTH	RACMO22E	r1i1p1	MPI-M-MPI-ESM-LR	REMO2009	r1i1p1
ICHEC-EC-EARTH	RACMO22E	r3i1p1	MPI-M-MPI-ESM-LR	REMO2009	r2i1p1
ICHEC-EC-EARTH	HadREM3-GA7-05	r12i1p1	MPI-M-MPI-ESM-LR	RCA4	r1i1p1
ICHEC-EC-EARTH	RCA4	r12i1p1	MPI-M-MPI-ESM-LR	RCA4	r2i1p1
ICHEC-EC-EARTH	RCA4	r1i1p1	MPI-M-MPI-ESM-LR	RCA4	r3i1p1
ICHEC-EC-EARTH	RCA4	r3i1p1	NCC-NorESM1-M	COSMO-crCLIM-v1-1	r1i1p1
IPSL-IPSL-CM5A-MR	HIRHAM5	r1i1p1	NCC-NorESM1-M	ALADIN63	r1i1p1
IPSL-IPSL-CM5A-MR	REMO2015	r1i1p1	NCC-NorESM1-M	HIRHAM5	r1i1p1
IPSL-IPSL-CM5A-MR	WRF381P	r1i1p1	NCC-NorESM1-M	REMO2015	r1i1p1
IPSL-IPSL-CM5A-MR	RACMO22E	r1i1p1	NCC-NorESM1-M	RegCM4-6	r1i1p1
IPSL-IPSL-CM5A-MR	RCA4	r1i1p1	NCC-NorESM1-M	WRF381P	r1i1p1
MIROC-MIROC5	CCLM4-8-17	r1i1p1	NCC-NorESM1-M	RACMO22E	r1i1p1
MIROC-MIROC5	REMO2015	r1i1p1	NCC-NorESM1-M	HadREM3-GA7-05	r1i1p1
MOHC-HadGEM2-ES	COSMO-crCLIM-v1-1	r1i1p1	NCC-NorESM1-M	RCA4	r1i1p1
MOHC-HadGEM2-ES	CCLM4-8-17	r1i1p1			